A study of the metal to nonmetal transition in Bi-doped β-PbO_2 by high resolution x-ray photoemission

S. Rothenberg, D. J. Payne, A. Bourlange, and R. G. Egdell[a)]
Department of Chemistry, University of Oxford, Inorganic Chemistry Laboratory, South Parks Road, Oxford OX1 3QR, United Kingdom

(Received 14 September 2007; accepted 12 October 2007; published online 12 December 2007)

The influence of Bi doping on the electronic structure of β-PbO_2 has been studied by high resolution x-ray photoemission spectroscopy. Doped films were prepared on Pt substrates by electrochemical deposition from solutions of $Pb(NO_3)_2$ and $Bi(NO_3)_3$ in HNO_3. Bi doping was found to lead to a lowering of the density of states at the Fermi energy in valence region x-ray photoemission and to suppression of final state screening by mobile conduction electrons in Pb $4f$ core level photoemission. A metal to nonmetal transition was found to occur for bulk doping levels around 5 at. % Bi. There is evidence of pronounced surface segregation of Bi. In contrast to host Pb ions, core holes on surface Bi ions do not couple to the mobile conduction electrons in the metallic state. It is concluded that Bi acts as a p-type acceptor in β-PbO_2 and traps charge carriers introduced by oxygen deficiency in PbO_{2-x}. © *2007 American Institute of Physics*. [DOI: 10.1063/1.2821362]

I. INTRODUCTION

Bi is widely used as a dopant in the PbO_2 coated anode plate of lead-acid batteries and appears to improve the capacity and charge acceptance capability of the battery, thereby prolonging life cycle.[1–3] Doping PbO_2 films with Bi also enhances their performance and durability in the anodic oxidation of organic species[4–9] such as phenols and in the oxidation of $(CH_3)_2SO$ to $(CH_3)_2SO_2$.[10] Despite the technological importance of Bi-doped PbO_2, very little attention has been devoted to the electronic effects of Bi doping in this system. In particular, there has been no work to date on this system by photoemission spectroscopy.

Electrochemically deposited PbO_2 is invariably a metallic conductor of electricity. Despite earlier suggestions[11] that metallic behavior is intrinsic to stoichiometric PbO_2, it has recently been established that metallic conductivity is associated with partial occupation of a conduction band of strongly hybridized Pb $6s-O\ 2p$ states that sits above the main valence band of the material.[12–14] Detailed analysis of the conduction band structure in photoemission indicates (albeit indirectly) that there is a small bandgap of order 0.7 eV between the valence and conduction bands.[14] Density functional bandstructure calculations performed within the framework of the generalized gradient approximation (GGA) show that the conduction band would be empty in stoichiometric PbO_2.[12–14] The conduction band occupancy must therefore arise from donor defects, probably oxygen vacancies. Based on this assumption it may be inferred from the measured conduction electron concentration that the oxygen deficiency parameter (x in PbO_{2-x}) is typically about 0.02 in as-deposited films, increasing to 0.04 in UHV annealed samples.[14] Bi is of course a group 15 element with a valence electron configuration $6s^26p^3$ in the free atom. Thus Bi has one more valence electron than the host group 14 element Pb, whose corresponding electron configuration is $6s^26p^2$. If Bi doping in PbO_{2-x} were to involve substitution of Bi(V) onto Pb(IV) sites to give $Pb_{1-y}Bi_yO_{2-x}$, Bi would act as a one electron donor in the absence of compensation by other defects. However, transport measurements reveal that Bi doping in electrochemically deposited PbO_2 films induces a transition to nonmetallic states, an observation that is completely at odds with this expectation.[15] The influence of Bi doping on PbO_2 is particularly puzzling given that Sb doping in SnO_2 leads to a well-defined increase in the carrier concentration, as expected for substitution of a group 15 element onto a host cation site previously occupied by a group 14 element.[16–18]

In the present paper we present a study of Bi-doped PbO_2 by high resolution x-ray photoemission spectroscopy. As in the earlier work, films were prepared by electrochemical deposition from acidic solutions of $Pb(NO_3)_2$ and $Bi(NO_3)_3$. However, in the earlier experiments[15] the compositions of the deposited films were not characterized and it was assumed that the bulk Bi doping level could be simply equated with the Bi/Pb ratio in solution. Here we pay particular attention to the bulk doping level that is actually achieved. It is shown that Bi doping in PbO_2 leads to a lowering of the density of states at the Fermi energy, with a transition to a nonmetallic state for bulk Bi doping levels greater than about 5 at. %. At the same time Bi doping suppresses the screening of core holes by mobile conduction electrons, leading to pronounced changes in the Pb $4f$ core lineshape. The reasons for the differing effect of Bi doping in PbO_2 from that of Sb doping in SnO_2 are discussed in detail.

II. EXPERIMENTAL PROCEDURE

Films of PbO_2 with a nominal thickness of about 15 μm were deposited on polished Pt disks by anodic oxidation of $0.4M$ $Pb(NO_3)_2$ in $0.1M$ HNO_3 at 60 °C.[19,20] For the first few seconds of deposition a high current density (~200 mA/cm^2) was used to encourage uniform nucleation across

[a)]Author to whom correspondence should be addressed. Electronic mail: russell.egdell@chem.ox.ac.uk.

the surface. After this initial pulse the current density was reduced to 10 mA/cm^2. Bi-doped samples were prepared by adding $Bi(NO_3)_3$ also dissolved in HNO_3 to the electrolyte solution before deposition. Samples with nominal Bi doping levels (as defined by the atomic Bi concentration in solution) of 0.5%, 1%, 2%, 5%, 10%, and 20% were prepared in this way. Radiofrequency inductively coupled plasma atomic emission spectroscopy was used to confirm that the concentration of Bi in the electrolyte solution corresponded to the nominal value. After deposition, films were removed from the solution, rinsed in ultrapure water, and then dried in an oven at a moderate temperature (~60 °C). The Bi-doped films were found to be much more brittle than the undoped films and required careful handling. The bulk Bi concentration was established by dissolving the films in concentrated nitric acid (15*M*), the weight loss due to dissolution being recorded. The resulting solution was diluted with further HNO_3 to give a Bi concentration of about 80 ppm. The Bi concentration was then determined by radiofrequency inductively coupled plasma atomic emission spectroscopy. For convenience the samples are identified in terms of the measured bulk doping level. It will be seen that both bulk and surface doping levels were much greater than the nominal doping level.

High-resolution x-ray photoemission spectra (XPS) were measured in a Scienta ESCA 300 spectrometer. This incorporates a rotating anode Al $K\alpha$ ($h\nu$=1486.6 eV) x-ray source, a seven crystal x-ray monochromator, and a 300 mm mean radius spherical sector electron energy analyzer with parallel electron detection system. The instrument resolution was 350 meV. Spectra were measured both for "as presented" samples and for samples which had been cleaned by annealing in UHV at 230 °C for 1 h in order to minimize the level of surface contamination by C. The annealing procedure had no significant effect on the surface Bi concentration in XPS and did not lead to any phase changes in the films as gauged by x-ray diffraction (XRD). However, as mentioned above *in situ* annealing does lead to a doubling of the carrier concentration for undoped PbO_2 with a concomitant increase in the intensity of photoemission at the Fermi energy by a factor of around $2^{1/3}$. For consistency all the data presented in the present paper relate to annealed samples. Binding energies were referenced to the Fermi energy of a silver foil regularly used to calibrate the spectrometer. The Fermi energies for the metallic samples studied in the current work were all coincident with the Fermi energy of the Ag reference.

III. RESULTS

A. Structure and chemical composition

Electrolytic deposition from acidic solutions containing $Pb(NO_3)_2$ and $Bi(NO_3)_3$ gave black adherent films whose x-ray powder diffraction patterns were dominated by reflections from the rutile β phase of PbO_2. For the undoped films diffraction weak peaks due to α-PbO_2 were also observed, but the α-phase reflections disappeared for even the lowest levels of Bi doping (Fig. 1). At the same time there were pronounced changes in the texture of the films with doping.

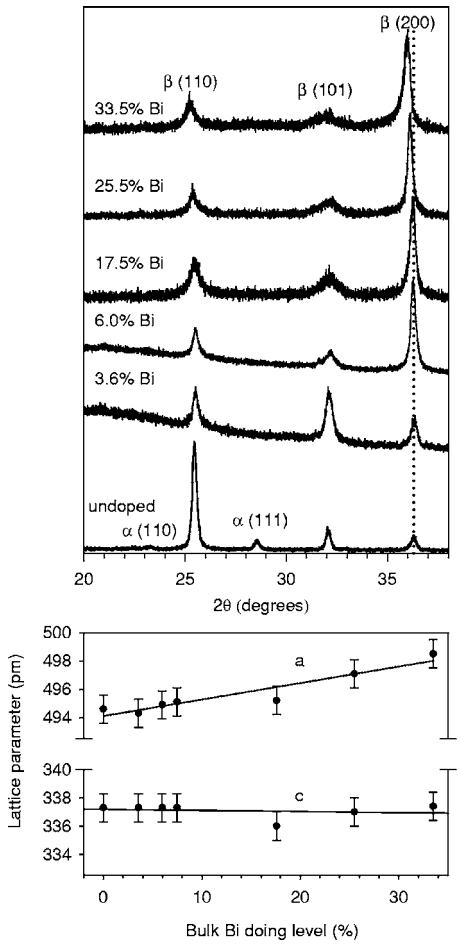

FIG. 1. Upper panel: partial powder x-ray diffraction scans of undoped and Bi-doped PbO_2 films. Note broadening and shift of diffraction peaks to low angle with Bi doping. Lower panel: tetragonal lattice parameters for β-PbO_2 phase as a function of bulk Bi doping level.

For undoped films the dominant reflection from the rutile phase was (110), but for the higher Bi doping level (200) reflection was predominant. In addition Bi doping led to pronounced broadening of the diffraction peaks and a shift of most reflections to low angle. From the shifts it may be estimated that the a lattice parameter for the tetragonal rutile phase increases from 4.946 to 4.985 Å for the film with 33.5% bulk Bi doping level (the highest studied). The *c* lattice parameter showed little variation with doping (Fig. 1).

Chemical analysis confirmed incorporation of Bi into the films, but the bulk doping level was always much greater than the nominal doping level as defined by the concentration of Bi in the solution used for electrolytic deposition (Table I), especially at the lower doping levels. Thus 0.5 at. % Bi in the electrolytic solution leads to a film with 3.6% Bi (as defined by the cation percentage) while 1% Bi gives 6.0% Bi in the film. These findings conflict with previous claims that there is no preferential incorporation of Bi into electrochemically deposited films.[15,21] However, in the earlier work electrochemical deposition was carried at room temperature and there was no direct measurement of the bulk doping levels. We found that films deposited at 60 °C were more robust and better suited to detailed spectroscopic investigation than samples deposited at room temperature.

TABLE I. Bulk and apparent surface Bi doping levels in electrochemically deposited PbO_2 films as a function of Bi cation % in the solution used for electrolytic deposition.

Bi in electrolyte (%)	Bulk Bi doping level (%)	Surface Bi level[a] (%)
0.5	3.6	21
1.0	6.0	24
2.0	7.5	33
5.0	17.6	44
10.0	25.5	44
20.0	33.5	47
30.0	38.0	···

[a]Defined as $[I(\text{Bi } 4f_{7/2})/S(\text{Bi } 4f_{7/2})]/[I(\text{Bi } 4f_{7/2})/S(\text{Bi } 4f_{7/2})+I(\text{Pb } 4f_{7/2})/S(\text{Pb } 4f_{7/2})]\times 100\%$ where the I are XPS intensities and the S are atomic sensitivity factors.

Core level XPS in the Bi+Pb $4f$ or $4d$ region showed very strong Bi core level signals (Figs. 2 and 3). After correction for atomic sensitivity factors, the $4f$ peak areas were used to derive effective surface concentrations of Bi. As shown in Table I, apparent surface Bi concentrations determined by XPS were greater than both the solution Bi concentration and the measured bulk doping level. This provides evidence for pronounced surface segregation of Bi in this system. The surface Bi doping level reached a value just under 45 cation % for solutions containing only 5% Bi and showed little further increase for solution concentrations up to 20% Bi. Unfortunately due to the rough morphology of the films it was not possible to use the variations in relative intensity of the core peaks with electron takeoff angle to explore the depth distribution of Bi. However, it is very striking that the increase of the intensity in the inelastic background is very small for the Bi $4f$ (Fig. 2) and Bi $4d$ peaks (Fig. 3) as compared with the Pb $4f$ and Pb $4d$ peaks. This suggests that most of the Bi intensity seen in XPS comes from Bi cations confined to the topmost ionic layers of the doped material. The photoelectrons emerging from these surface Bi ions can escape into the vacuum without suffering inelastic energy loss and hence the inelastic background is very weak. Assuming a separation of 3.5 Å between cation containing layers [this is the separation between (110) cation containing planes] and an inelastic mean free path of about 15 Å for Pb and Bi $4f$ photoelectrons, the XPS intensity ratio for samples with bulk Bi doping levels of 3.6% and 6.0% can

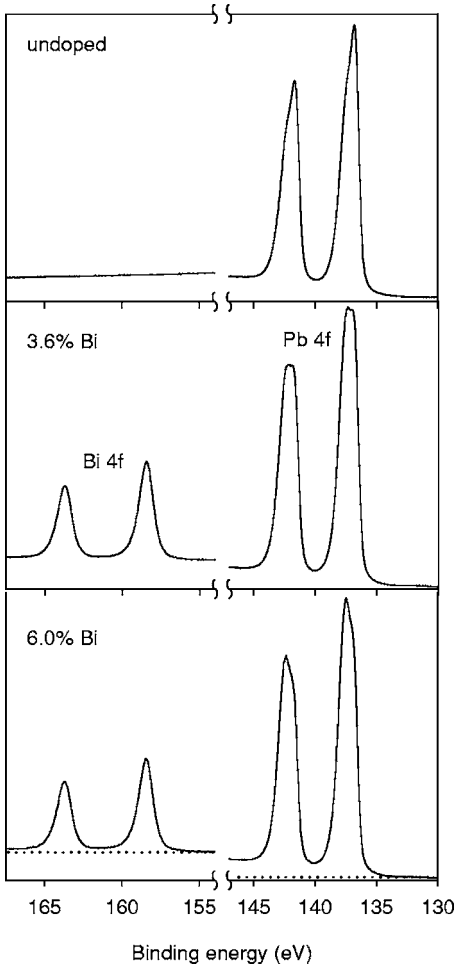

FIG. 2. Pb $4f$ and Bi $4f$ core level structures in undoped PbO_2 and in Bi-doped PbO_2 films prepared from solutions containing 0.5% and 1% Bi, corresponding to 3.6% and 6.0% bulk Bi doping. The dotted baseline emphasizes the weakness of the inelastic background associated with the Bi $4f$ core levels.

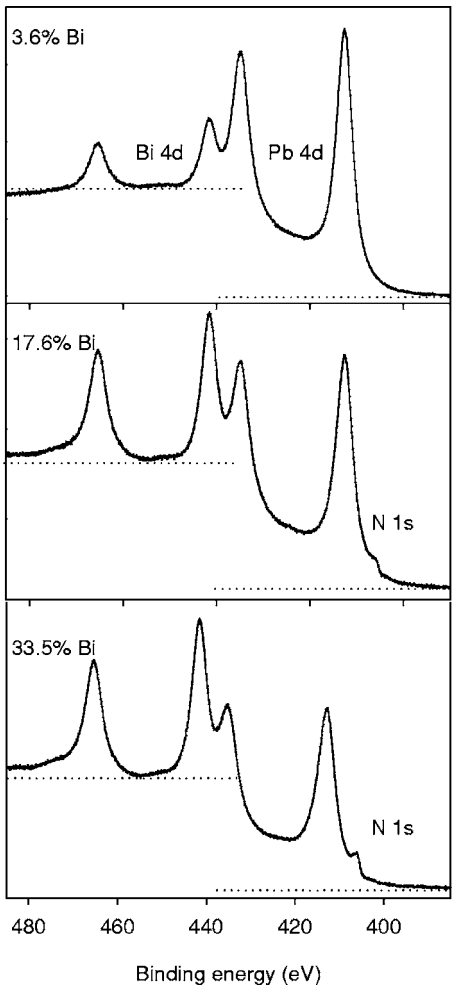

FIG. 3. Pb $4d$ and Bi $4d$ core level structures in Bi-doped PbO_2 films prepared from solutions containing 1%, 5%, and 20% Bi, corresponding to 3.6%, 6.0%, and 33.5% bulk Bi doping. The dotted line emphasizes the weakness of the inelastic background associated with the Bi $4d$ core level. Note the appearance of a N $1s$ peak in the two lower spectra.

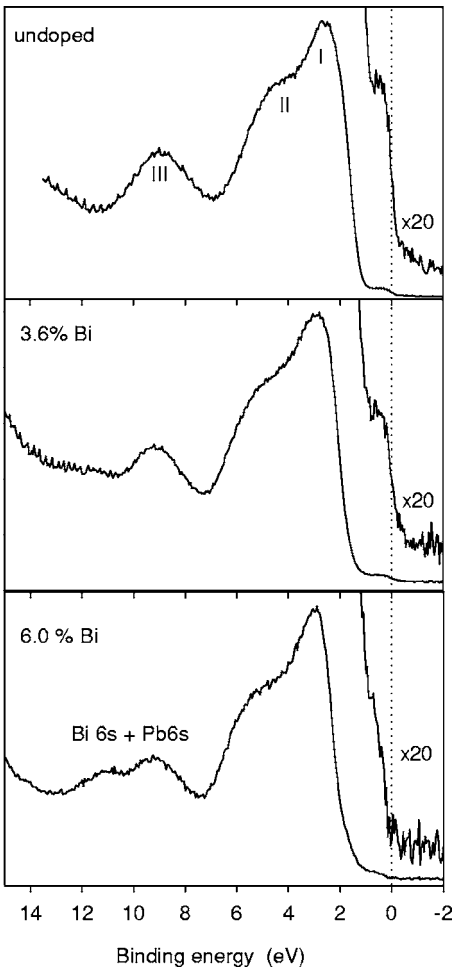

FIG. 4. Valence band XPS of undoped PbO_2 and Bi-doped PbO_2 films prepared from solutions containing 0.5% and 1% Bi.

be explained satisfactorily in terms of a surface cation layer exclusively containing Bi ions, with an abrupt return to the bulk doping level in the next and subsequent ionic layers. Thus XPS is *not* probing a surface region homogenously enriched in Bi. Similar behavior in the inelastic background has been observed before in Ba-doped MgO,[22] where Ba segregation is driven by the large size of Ba as compared with Mg. Segregation has also been observed in the closely related system Sb-doped SnO_2. Here accumulation of Sb in the topmost ionic layer is driven by the ease of accommodation of "lone pair" Sb(III) ions in surface sites.[16–18] Deposition from solutions containing 5% Bi or more led to incorporation of N into the films, probably as nitrate species. This is evidenced by the appearance of a N 1*s* peak at a binding energy of 406.2 eV which appears as a weak feature on the side of the stronger Pb $4d_{5/2}$ peak. For this reason detailed discussion of changes in electronic structure due to Bi doping is confined to samples prepared from solutions containing less than 5% Bi.

B. Electronic structure

Valence band x-ray photoemission spectra of nominally undoped PbO_2 and of samples with 3.6% and 6.0% bulk Bi doping are shown in Fig. 4. In agreement with previous work, the spectrum of PbO_2 contains three principal bands I–III.[12–14] The spectral profile mirrors that from GGA density functional calculations[12–14] show that band I is of dominant O 2*p* atomic character while band II contains a pronounced Pb 5*p* contribution. Hard x-ray photoemission and O *K* shell x-ray emission spectroscopies show that the states at the bottom of the valence band in III are of dominant Pb 6*s* atomic character with minority admixture of O 2*p* states.[13] Close to the Fermi energy is a further weak feature which terminates in Fermi-Dirac-like cutoff. This corresponds to conduction band states populated due to donor defects. In principle both proton interstitials and oxygen vacancies could act as donors, but we have recently established from time of flight neutron diffraction that as prepared PbO_2 contains a significant number of oxygen vacancies.[23]

Bi doping produces only minor changes in the upper part of the valence band spectrum, but a new feature appears to high binding energy of band III. This corresponds to Bi 6*s* states and is at an energy similar to a related band of dominant Bi 6*s* character in Bi_2O_3.[24] The significant differences in this spectral region between samples with 3.6% and 6% bulk Bi doping are somewhat surprising given the relatively small increase in surface Bi concentration (Table I). However, in moving from the lower to the higher doping level one crosses a metal insulator transition and this may also influence the spectral profile in this region. Most striking, however, is that even at the lowest Bi doping level studied there is a lowering in the intensity of the Fermi level cutoff. For samples with a bulk doping level of 6.0% Bi or higher, the density of states at the Fermi energy is close to zero, signaling a Bi-induced transition to a nonmetallic state.

The changes in the valence band spectra are accompanied by profound changes in the Pb 4*f* core level spectra as shown in Fig. 5. Here it can be seen that the Pb $4f_{7/2}$ core level spectrum of nominally undoped PbO_2 consists of two overlapping components. Fitting the spectral profile to two pseudo-Voigt functions shows that the spectrum is built up from a relatively narrow and dominantly Gaussian low binding energy component and a broader and dominantly Lorentzian component to high binding energy. Bi doping leads to suppression in the intensity of the low binding energy component of the spectra. The two peak structure can be understood in terms of the model proposed by Kotani and Toyazawa[25] for core ionization in a narrow band metallic system, as shown schematically in Fig. 6. The Coulomb potential associated with the core hole pulls a localized state below the conduction band on the ionized atom. Two different final states are then possible depending on whether the localized trap state is filled by an electron from the conduction band to give a screened final state or remains empty to give an unscreened final state. The core level structure thus comprises a low binding energy component associated with the screened final state and a lifetime broadened high binding energy component with a predominantly Lorentzian lineshape associated with the unscreened final state. Structure similar to that in Fig. 6 has been observed previously for a number of other metallic post-transition metal oxide systems, including Sb-doped SnO_2,[26,27] Sn-doped In_2O_3,[28,29] and Tl_2O_3.[30] The evolution of spectral structure with Bi doping therefore indicates that there is a progressive decrease in the

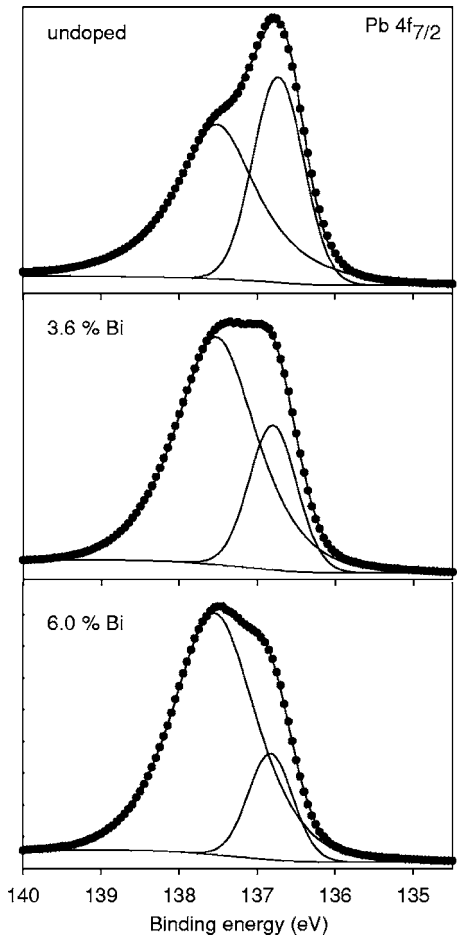

FIG. 5. Pb $4f_{7/2}$ core level structure in XPS of undoped PbO_2 and Bi-doped PbO_2 films prepared from solutions containing 0.5% and 1% Bi. The core lines have been fitted to a Shirley background and a pair of pseudo-Voigt functions.

probability of final state screening. This parallels the progressive decrease in the density of states at the Fermi enegy with increasing Bi doping, as would be expected. It is perhaps puzzling that the screened final state component does not disappear completely in the 6.0% Bi-doped sample even though there appears to be a vanishing density of states at the Fermi energy in this material. However, if the Coulomb potential associated with the core hole is bigger than the effective gap between filled and empty states then core hole screening should still be possible. This idea is discussed further below.

In contrast to the Pb 4*f* core levels, the Bi 4*f* core levels gave simple lineshapes that could be fitted to a single pseudo-Voigt component (Fig. 7). It follows that the majority of the Bi probed by XPS sits in sites not subject to final state screening by mobile conduction electrons. This conclusion is in turn consistent with the hypothesis that the Bi core level signals in XPS are dominated by ions occupying surface or grain boundary sites rather than ions occupying bulk substitutional sites. These surface ions couple only weakly to the bulk conduction electron gas and in our discussion below we assume that the surface segregated Bi ions do not influence the metal to nonmetal transition revealed by valence region x-ray photoemission.

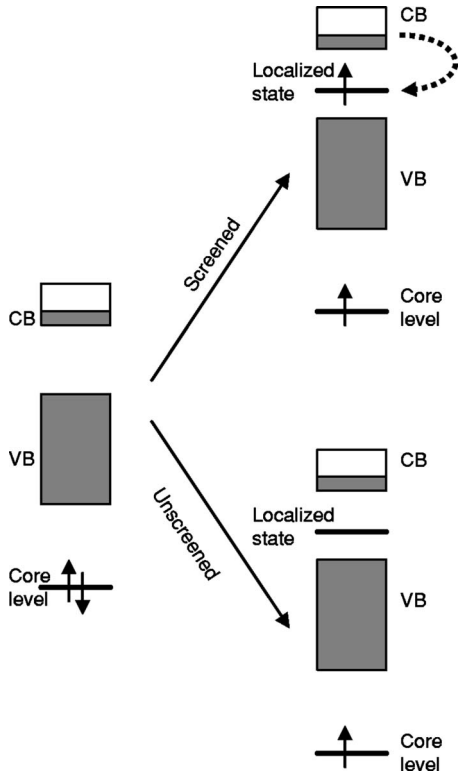

FIG. 6. Schematic representation of final state screening of a core hole in a narrow band metallic material as described by Kotani and Toyazawa's model.

IV. DISCUSSION

The observation of a metal to nonmetal transition with Bi doping is consistent with earlier transport measurements[15] which revealed that undoped electrochemically deposited PbO_2 films exhibited metallic conductivity but that material

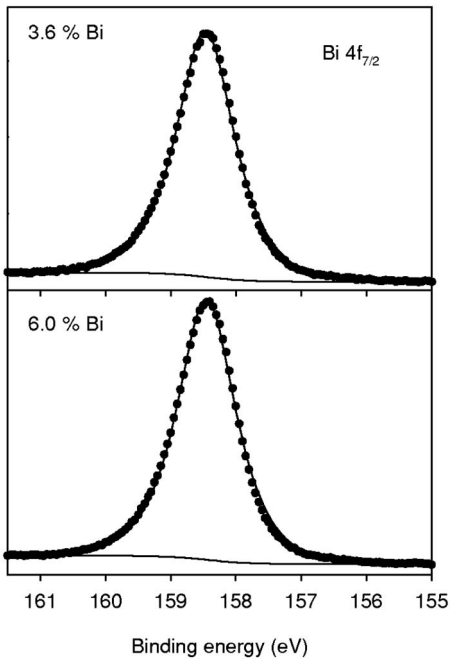

FIG. 7. Bi $4f_{7/2}$ core level structure in XPS of Bi-doped PbO_2 films prepared from solutions containing 0.5% and 1% Bi. The core lines have been fitted to a Shirley background and a single pseudo-Voigt function.

prepared from solutions containing 20% and 30% Bi were nonmetallic, with a resistivity ρ that increased with decreasing temperature T according to a power law of the form $\rho \propto T^{-p}$ where p equaled 0.26 and 0.49, respectively, for the 20% and 30% samples. The present work pinpoints the onset of nonmetallic behavior at a lower doping level than implied by the previous work, although it should be noted that no transport measurements were reported in the earlier work for nominal doping levels between 0% and 20% Bi.

The influence of Bi doping in PbO_2 differs markedly from that of Sb doping in SnO_2, even though Pb and Bi lie immediately below Sn and Sb in the Periodic Table. The host oxide SnO_2 can easily be prepared as a stoichiometric and insulating material. Sb doping leads to the onset of metallic conductivity. This is accompanied by the development of a distinct conduction band feature in ultraviolet[16–18] or x-ray photoemission[27] spectroscopy, the appearance of plasmon peaks in electron energy loss[16–18] or infrared reflection[31,32] spectra, and the emergence of structure in core level x-ray photoemission spectra attributable to metallic final state screening.[26,27] In this system antimony substitutes into Sn(IV) sites as Sb(V) and charge balance is maintained by introduction of itinerant electrons into the conduction band. Although Sb(V) has a smaller ionic radius than Sn(IV),[33] the conduction band states are Sn–O antibonding and there is a small overall increase in lattice parameter with Sb doping.[32,34] In ceramic samples of Sb-doped SnO_2 there is also evidence of pronounced segration of Sb to surface or grain boundary sites.[16–18] The surface Sb ions occupy noncentrosymmetic sites where hybridization between Sb 5*s* and 5*p* levels is mediated by mutual interaction with anion O 2*p* states thus allowing the Sb ions to trap electrons in 5*s*-5*p* hybrid lone pair to give surface Sb(III) ions. These may be identified in Mössbauer spectroscopy.[35]

Due largely to relativistic effects, Bi 6*s* electrons have a higher binding energy than Sb 5*s* electrons. This in turn is reflected in the chemistry of the two elements. In particular, the group oxidation state for Bi is much less widespread and much more strongly oxidizing than the group oxidation state for Sb. For example, "Bi_2O_5" is an ill-characterized compound of marginal stability at room temperature, but Sb_2O_5 is a well-defined monoclinic solid.[36–38] We therefore suggest that Bi substitutes into PbO_2 as Bi(III) rather than Bi(V). In this oxidation state Bi acts as a *p*-type acceptor rather than as an *n*-type donor. The acceptor centers will compensate the donor states introduced by oxygen vacancies in PbO_{2-x}, each Bi(III) trapping one conduction band electron. Charge balance can be maintained up to the composition $Pb(IV)_{1-2x}Bi(III)_{2x}O_{2-x}$ at which point the carrier concentration has been reduced to zero. Alternatively we may envisage coexistence of the two Bi valence states as in $BaBiO_3$, in which case a higher Bi concentration would be required to compensate the *n*-type doping due to O vacancies. We note that the Bi concentration in the nonmetallic 6% Bi-doped sample is 1.4×10^{21} cm^{-3}, as compared with an estimated carrier concentration of about 2×10^{21} cm^{-3} for an UHV annealed PbO_2 film.[14] A transition to a nonmetallic state may, however, be induced before the Bi concentration reaches the initial free electron concentration due to the disorder associated with the Bi dopant atoms, leading to Anderson localization. The observation of states above the main valence band edge in the photoemission spectrum of the nonmetallic sample supports this idea. In any case the relatively low doping level needed to supress metallic behavior suggests that substitution is mainly as Bi(III). Incorporation of further Bi beyond $Pb(IV)_{1-2x}Bi(III)_{2x}O_{2-x}$ requires compensation by an increased oxygen vacancy concentration as in $Pb(IV)_{1-2x-y}Bi(III)_{2x+y}O_{2-x-y/2}$ or cosubstitution of Bi(III) and Bi(V) as discussed above. The hypothesis of Bi(III) substitution is, however, consistent with the very pronounced increase in the *a* lattice parameter with Bi doping. The Shannon ionic radius of six-coordinate Bi(III) is quoted as 103 pm, much bigger than the value of 77 pm for Pb(IV) or 76 pm for Bi(V).[33] However, further experimental work using neutron diffraction is necessary to establish if Bi doping at high levels introduces oxygen vacancies beyond those found in undoped material.

V. CONCLUDING REMARKS

The influence of Bi doping on the electronic structure of PbO_2 has been studied in films electrochemically deposited on Pt substrates. Bi doping is found to induce a metal to nonmetal transition whose spectroscopic signatures are (i) a suppression of the density of states at the Fermi energy in valence region photemission and (ii) a reduced probability of final state screeing in Pb 4*f* core level photoemission. The transition is associated with incorporation of Pb into the PbO_2 lattice as Bi(III) rather than Bi(V) so that the dopant acts as a *p*-type acceptor which compensates the *n*-type doping asociated with oxygen deficiency in PbO_2 itself. The differing influences of the group 15 dopant in Bi-doped PbO_2 and Sb-doped SnO_2 are consistent with the broader chemical differences between Bi and Sb. The Bi doping level required to induce the metal to nonmetal transition in PbO_2 is much greater than the doping levels used to to improve the durability of anode coatings in lead-acid batteries.[1–3] We may conclude that the improved functional performance induced by Bi doping is not directly related to the metal to the nonmetal transition. However, the pronounced tendency of Bi to segregate to surface sites will be expected to have a strong influence on surface energies, which may in turn influence the microstructure of the PbO_2 in anode coatings.

ACKNOWLEDGMENTS

A.B. acknowledges support from EPSRC under Grant No. GR/S94148. The NCESS facility at Daresbury Laboratory was supported by EPSRC Grant No. GR/S14252. We thank Dr. G. Beamson and Dr. D. S. L. Law for help with the photoemission measurements.

[1] L. T. Lam, O. V. Lim, N. P. Haigh, D. A. J. Rand, J. E. Manders, and D. M. Rice, J. Power Sources **73**, 36 (1998).
[2] L. T. Lam, N. P. Haigh, and D. A. J. Rand, J. Power Sources **88**, 11 (2000).
[3] H. Y. Chen, L. Wu, C. Ren, Q. Z. Luo, Z. H. Xie, X. Jiang, S. P. Zhu, Y. K. Xia, and Y. R. Luo, J. Power Sources **95**, 108 (2001).
[4] Y. Mohd and D. Pletcher, J. Electrochem. Soc. **152**, D97 (2005).
[5] K. T. Kawagoe and D. C. Johnson, J. Electrochem. Soc. **141**, 3404 (1994).
[6] C. Borras, T. Laredo, J. Mostany, and B. R. Scharfker, Electrochim. Acta **48**, 2775 (2003).

[7]C. Borras, T. Laredo, J. Mostany, and B. R. Scharfker, Electrochim. Acta **49**, 641 (2004).
[8]S. E. Treimer, J. R. Feng, M. D. Scholten, D. C. Johnson, and A. J. Davenport, J. Electrochem. Soc. **148**, 459(E) (2001).
[9]N. D. Propovic, J. A. Cox, and D. C. Johnson, J. Electroanal. Chem. **455**, 153 (1998).
[10]H. P. Chang and D. C. Johnson, Anal. Chim. Acta **248**, 85 (1991).
[11]M. Heinemann, H. J. Terpstra, C. Haas, and R. A. de Groot, Phys. Rev. B **52**, 11740 (1995).
[12]D. J. Payne, R. G. Egdell, W. Hao, J. S. Foord, A. Walsh, and G. W. Watson, Chem. Phys. Lett. **411**, 181 (2005).
[13]D. J. Payne, R. G. Egdell, G. Paolicelli, F. Offi, G. Panaccione, P. Lacovig, G. Monaco, G. Vanko, A. Walsh, G. W. Watson, J. Guo, G. Beamson, P.-A. Glans, T. Learmonth, and K. E. Smith, Phys. Rev. B **75**, 153102 (2007).
[14]D. J. Payne, R. G. Egdell, D. S. L. Law, P.-A. Glans, T. Learmonth, K. E. Smith, J. Guo, A. Walsh, and G. W. Watson, J. Mater. Chem. **17**, 267 (2007).
[15]W. T. Fu and H. C. F Martens, Solid State Commun. **115**, 423 (2000).
[16]P. A. Cox, R. G. Egdell, A. F. Orchard, C. Harding, W. R. Patterson, and P. Tavener, Solid State Commun. **44**, 837 (1982).
[17]P. A. Cox, R. G. Egdell, C. Harding, W. R. Patterson, and P. Tavener, Surf. Sci. **123**, 179 (1982).
[18]R. G. Egdell, W. R. Flavell, and P. Tavener, J. Solid State Chem. **51**, 345 (1984).
[19]A. B. Velichenko, R. Amadelli, A. Benedetti, D. V. Girendko, S. V. Kovalyov, and F. I. Danilov, J. Electrochem. Soc. **149**, C445 (2002).
[20]S. Abaci, K. Pekmez, T. Hokelek, and A. Yildiz, J. Power Sources **88**, 232 (2000).
[21]J. S. Gordon, V. G. Young, and D. C. Johnson, J. Electrochem. Soc. **141**, 652 (1994).
[22]M. Cotter, S. Campbell, L. L. Cao, R. G. Egdell, and W. C. Mackrodt, Surf. Sci. **208**, 267 (1989).
[23]D. J. Payne, M. O. Jones, and R. G. Egdell (in preparation).
[24]D. J. Payne, R. G. Egdell, A. Walsh, G. W. Watson, J. Guo, P. A. Glans, T. Learmonth, and K. E. Smith, Phys. Rev. Lett. **96**, 157403 (2006).
[25]A. Kotani and Y. Toyazawa, J. Phys. Soc. Jpn. **37**, 912 (1974).
[26]R. G. Egdell, J. Rebane, T. J. Walker, and D. S. L. Law, Phys. Rev. B **59**, 1792 (1999).
[27]R. G. Egdell, T. J. Walker, and G. Beamson, J. Electron Spectrosc. Relat. Phenom. **128**, 59 (2003).
[28]V. Christou, M. Etchells, O. Renault, P. J. Dobson, O. V. Salata, G. Beamson, and R. G. Egdell, J. Appl. Phys. **88**, 5180 (2000).
[29]Y. Gassenbauer, R. Schafranek, and A. Klein, Phys. Rev. B **73**, 245312 (2006).
[30]P. A. Glans, T. Learmonth, K. E. Smith, J. Guo, A. Walsh, G. W. Watson, F. Terzi, and R. G. Egdell, Phys. Rev. B **71**, 235109 (2005).
[31]C. S. Rastomjee, P. A. Cox, R. G. Egdell, J. P. Kemp, and W. R. Flavell, J. Mater. Chem. **1**, 451 (1991).
[32]Z. C. Orel, B. Orel, M. Hodoscek, and V. Kaucic, J. Mater. Sci. **27**, 313 (1992).
[33]R. D. Shannon, Acta Crystallogr., Sect. A: Cryst. Phys., Diffr., Theor. Gen. Crystallogr. **32**, 751 (1976).
[34]T. Kikuchi and M. Umehara, J. Mater. Sci. Lett. **4**, 1051 (1985).
[35]F. J. Berry and C. Greaves, J. Chem. Soc. Dalton Trans. **1981**, 2447.
[36]F. A. Cotton, G. Wilkinson, C. A. Murillo, and M. Bochmann, *Advanced Inorganic Chemistry*, 6th ed. (Wiley, New York, 1999).
[37]A. F. Wells, *Structural Inorganic Chemistry*, 5th ed. (Clarendon, Oxford, 1990).
[38]M. Jansen, Acta Crystallogr., Sect. B: Struct. Crystallogr. Cryst. Chem. **35**, 539 (1979).